# Systemic analysis of tissue cells potentially vulnerable to SARS-CoV-2 infection by the protein-proofed single-cell RNA profiling of ACE2, TMPRSS2 and Furin proteases

Lulin Zhou[1, 2 §], Zubiao Niu[1§], Xiaoyi Jiang[1, 4 §], Zhengrong Zhang[1], You Zheng[1], Zhongyi Wang[1], Yichao Zhu[1], Lihua Gao[1], Xiaoning Wang[2, 3 *], Qiang Sun[1 *]

[1] Institute of Biotechnology, 20 Dongda Street, Beijing 100071, P.R. China.

[2] School of Medicine, Nankai University, 94 Weijin Road, Tianjin, 300071, P. R. China.

[3] National Clinic Center of Geriatric, the Chinese PLA General Hospital, Beijing 100853, P. R. China & School of Laboratory Medicine and Biotechnology, Southern Medical University, Guangzhou 510515, P. R. China

[4] Department of Oncology, Beijing Shijitan Hospital of Capital Medical University, 10 TIEYI Road, Beijing 100038, P. R. China;

§ Equal contribution

* To whom correspondence should be addressed. Tel: 86 10 66948818; Email: sunq@bmi.ac.cn.

Correspondence may also be addressed to Xiaoning Wang, Email: xnwang88@163.com.

**ABSTRACT**

Single-cell RNA profiling of ACE2, the SARS-CoV-2 receptor, had proposed multiple tissue cells as the potential targets of SARS-CoV-2, the novel coronavirus causing the COVID-19 pandemic. However, most were not echoed by the patients' clinical manifestations, largely due to the lack of protein expression information of ACE2 and co-factors. Here, we incorporated the protein information to analyse the expression of ACE2, together with TMPRSS2 and Furin, two proteases assisting SARS-CoV-2 infection, at single cell level in situ, which we called protein-proofed single-cell RNA (pscRNA) profiling. Systemic analysis across 36 tissues revealed a rank list of candidate cells potentially vulnerable to SARS-CoV-2. The top targets are lung AT2 cells and macrophages, then cardiomyocytes and adrenal gland stromal cells, followed by stromal cells in testis, ovary and thyroid. Whereas, the polarized kidney proximal tubule cells, liver cholangiocytes and intestinal enterocytes are less likely to be the primary SARS-CoV-2 targets as ACE2 localizes at the apical region of cells, where the viruses may not readily reach. These findings are in concert with the clinical characteristics of prominent lung symptoms, frequent heart injury, and uncommon intestinal symptoms and acute kidney injury. Together, we provide a comprehensive view on the potential SARS-CoV-2 targets by pscRNA profiling, and propose that, in addition to acute respiratory distress syndrome, attentions should also be paid to the potential injuries in cardiovascular, endocrine and reproductive systems during the treatment of COVID-19 patients.

**KEY WORDS:**

**COVID-19; SARS-CoV-2; ACE2; TMPRSS2; Furin; single cell RNA profiling; pscRNA profiling**

## INTRODUCTION

In January, 2020, a novel coronavirus of unknown origin was identified to cause severe pneumonia in about 15-20% infected patients [1, 2], the disease is currently called COVID-19 abbreviated from Coronavirus Disease 2019 [3]. The virus is phylogenetically similar (~76% amino acid identity) to the severe acute respiratory syndrome coronavirus (SARS-CoV) [4-8], and was subsequently named as SARS-CoV-2 after the initial name of 2019-nCoV. The SARS-CoV-2 virus is much more contagious than SARS-CoV, and had infected more than 679,000 cases of COVID-19 from 199 countries and territories by March 29, 2020, leading to more than 30 thousands of deaths with an average motility rate of about 4.6% [9]. The pandemic of COVID-19 is posing a global health emergency.

The coronavirus is a large group of enveloped, single-strand positive-sense RNA viruses, with SARS-CoV and Middle East respiratory syndrome coronavirus (MERS-CoV) the two known deadly viruses for human [10]. The spike (S) envelope glycoproteins on coronavirus are the major determinants of host cell entry. Proteolytic cleavage of S protein produces S1, the N-terminal region of S protein that is responsible for receptor binding, and S2, the trans-membrane C-terminal region of S protein that promotes membrane fusion. The cleavage step is often permissive for the fusion function of S protein as it helps to release the fusion peptide to insert into the target cellular membrane [10, 11]. Therefore, the host range and cell/tissue tropism of coronaviruses were believed to be controlled by the S protein engagement of host cell receptor, and by the proteolytic cleavage of the S protein as well [11]. Recently, works from several groups demonstrated, either bioinformatically or experimentally, that angiotensin-converting enzyme 2 (ACE2), the receptor for SARS-CoV virus [12], is also a functional cellular receptor for SARS-CoV-2 virus [6, 7, 13-15], and transmembrane protease serine 2 (TMPRSS2) and Furin are two proteases that process SARS-CoV-2 S protein to establish efficient infection [13, 14, 16, 17].

Single-cell RNA (scRNA) profiling is a state-of-the-art tool to dissect gene expression at single cell level, therefore was employed to explore the target cells of the SARS-CoV-2. Based on the profiling of ACE2 mRNA expression in different tissues/organs, multiple types of cells were proposed to be potentially targeted by SARS-CoV-2 virus, including the lung alveolar type 2 (AT2) cells [18], nasal epithelial cells [19], esophageal epithelial cells and intestinal enterocytes [20], liver cholangiocytes [21], cardiomyocytes [22], kidney proximal tubule cells [23], spermatogonia and Leydig/sertoli cells in testis [24]. However, unparallel to the many potential targets cells and organs proposed, the COVID-19 patients primarily displayed typical symptoms of inflammation in lung, where only a very small portion of cells (~0.64% of total cells, and ~1.4% of AT2 cells) expressed ACE2 mRNA [18]; meanwhile, the injuries in other organs/tissues, such as kidney and the intestinal track where ACE2 RNA expressed at high levels, seemed to be uncommon [1, 25]. This obvious discrepancy suggests that mechanisms other than ACE2 mRNA levels are also involved in the regulation of SARS-CoV-2 infection of their target cells.

Considering that mRNA level does not always dictate comparable protein expression, and subcellular localizations, which are missing information from mRNA profiling, are critical for protein functions, we set out to explore ACE2 expression at both mRNA and protein levels by taking advantages of the curated public database. We called this method as protein-proofed scRNA (pscRNA) profiling. Moreover, we also analysed the co-expression of ACE2 with its two processing proteases, TMPRSS2 and Furin, at single cell resolution in situ by pscRNA profiling. Systemic analysis of 36 human tissues/organs revealed that 1) a rank list of potential SARS-CoV-2 targets with lung AT2 cell and macrophages as the top targets, then cardiomyocytes, and stromal cells in testis, ovary, adrenal and thyroid glands. Among them, the lung macrophages, stromal cells in ovary and adrenal gland, were identified for the first time, which may account for severe clinical symptoms and rapid disease progression; 2) the mRNA levels may differ dramatically from the protein levels for ACE2, TMPRSS2 and Furin in different tissue cells; and protein subcellular localization is another factor potentially affecting virus host-entry; 3) the co-expression of ACE2 with TMPRSS2 and Furin proteases may contribute to establish efficient infection of SARS-CoV-2 virus.

## MATERIAL AND METHODS

### Data Acquisition

For scRNA profiling, the raw gene expression matrices for single cells were downloaded from Gene Expression Omnibus (GEO) database(https://www.ncbi.nlm.nih.gov/geo/) and Human Cell Atlas Data Portal (https://data.humancellatlas.org/). We totally acquired the single cell gene expression datasets of various normal tissues and organs, including lung, heart, liver, kidney, intestine, stomach, testis, ovary, adrenal gland and thyroid. Apart from the heart dataset that was obtained by the smart-seq2 method, a majority of the single cell data were generated through the 10x Chromium platform. The GEO accession number of these datasets respectively is GSE122960(lung) [26], GSE109816(heart) [27], GSE131685(kidney) [28], GSE125970(intestine) [29], GSE134520(stomach) [30], GSE109037(testis) [31], GSE134355(thyroid and adrenal gland)[32], and GSE118127(ovary) [33]. The liver dataset was acquired from the Human Cell Atlas Data Portal[34].

For tissue distribution of mRNA and protein expression profiles, data were obtained for target genes from the "TISSUE" categories of "THE HUMAN PROTEIN ATLAS" (http://www.proteinatlas.org/) [35]. The mRNA expression from GTEx dataset were chosen for demonstration with reference to the normalized consensus dataset [36]. The protein expression scores were extracted from the "PROTEIN EXPRESSION SUMMARY" subcategory. Immunohistochemistry (IHC) staining was performed on normal human tissue samples [37]. ACE2 expression were primarily detected with rabbit antibody (1:250, HPA000288, Sigma-Aldrich) and confirmed with mouse antibody (1:5000, CAB026174, R&D Systems); TMPRSS2 expression were detected with rabbit antibody (1:300, HPA035787, Sigma-Aldrich); Furin expression were detected with rabbit antibody (1:125, sc-20801, Santa Cruz Biotechnology). The information on expression intensity and cell types expressing respective genes were extracted from the staining reports for each staining in the database.

### Quality Control and Data Normalization

The raw count matrices were imported into R (version3.6.1, https://www.r-project.org/) and processed by the Seurat R package(version3.1.4)[38]. The filter criteria of low-quality cells were determined on the basis of the number of genes and the percentage of mitochondrial genes in the distinct tissue samples. Generally, cells with less than 200 detected genes, higher than 2500 detected genes and higher than 25% mitochondrial genome transcript ratio were removed. Specially, cells with higher than 72% mitochondrial genome transcript ratio in the heart dataset and cells with higher than 50% mitochondrial genome transcript ratio in the liver dataset were removed as mentioned by the corresponding authors[27, 34]. Then, the gene expression matrices were normalized and scaled. Briefly, for each cell, the expression counts for each gene were divided by the sum of counts for all genes of that cell, multiplied by a scaling factor (10, 000) and log transformed using the "Normalize Data" function in the R package Seurat. Furthermore, 2000 highly variable genes were selected based on a variance stabilizing transformation method for downstream analysis.

### Data Integration and Dimension Reduction

To avoid batch effects among samples and experiments in the heart and intestine datasets, we adopted the anchoring procedure in the Seurat R package to integrate the datasets as described previously [38]. In brief, the "anchor" correspondences between datasets were identified using the "Find Integration Anchors" function with default parameters in Seurat. And then, we used the "Integrate Data" function in Seurat to obtain the batch-corrected expression matrices. we also applied another integration approach called "Harmony"[39] to the kidney and testis datasets. The Harmony R package (version1.0, https://github.com/immunogenomics/Harmony) focuses on scalable integration of the scRNA-seq data for batch correction.

In order to reduce the number of dimensions representing each cell, the "Run PCA" functions in Seurat was performed to calculate principal components (PCs). And the number of PCs used in downstream analysis and visualization was determined based on the "Jack Straw" procedure and elbow of a scree plot. Nonlinear dimensionality reduction algorithms including uniform manifold approximation and projection (UMAP) and t-

distributed stochastic neighbour embedding (t-SNE) were also used to unsupervised clustering of single cells. Specifically, we made use of the UMAP and t-SNE to place cells with similar local neighbourhoods based on the statistically significant PCs to visualize the datasets.

**Cell Clustering, Annotation and Visualization**

We applied a graph-based clustering approach to assemble cells. Briefly, we constructed a K-nearest neighbour graph based on the Euclidean distance in principal component analysis(PCA) space and refined the edge weights between any two cells based on the shared overlap in their local neighbourhoods through the "Find Neighbors" function in Seurat. Subsequently, we applied the Louvain algorithm using the "Find Cluster" function in Seurat to group cells.

We applied two strategies to determine cell types. (1) Canonical marker genes were applied to annotate each cluster into known biological cell types. Expression dot plots or heatmaps of the marker genes for each cluster are shown in Figure 3. (2) We used the "Find All Markers" function from R package Seurat to find differentially expressed genes by comparing each cluster of cells with all other cells. Differentially expressed genes in each cluster were enriched to the cell markers gene sets[40] using the "Cluster Profiler" R package (version3.14.3) [41] to predict the probable cell types.

Umap plots, heatmaps, violin plots, and dot plots were generated using R package Seurat. In order to visualize co-expression of two genes simultaneously, we adopted the "Feature Plot" function and "Feature Scatter" function in Seurat. The typical execution is "Feature Plot" (data, features, blend = TRUE).

**RESULTS**

**Tissue distribution of ACE2, TMPRSS2 and Furin proteases**

Based on the expression analysis across 36 human tissues, ACE2 displays a tissue-specific expression at both mRNA and protein levels. And 10 tissues express relatively higher level of ACE2 mRNA, including small intestine, colon, esophagus, thyroid gland, kidney, testis, ovary, breast, heart muscle and adipose tissue. Meanwhile, the majority of the other tissues, such as lung, liver, pancreas, spleen, prostate, urinary bladder, skin and neuronal tissues, give marginal expression of ACE2 mRNA (Figure 1A-B, S1A). The protein expression score, though also displaying a tissue-specific pattern, only reports 6 tissues expressing ACE2 protein, with 5 of them matching the mRNA expression, including small intestine, colon, thyroid gland, kidney and testis. Interestingly, adrenal gland expresses, though little mRNA, median level of ACE2 protein. The inconsistency is actually also applied for ACE2 to other tissues such as breast, heart muscle and adipose tissue, which express high level of mRNA but undetectable protein.

The expression of TMPRSS2 also shows a tissue-specific pattern, but is different from that of ACE2 in terms of tissue distribution (Figure 1A, 1C, S1B and S1E). And 5 tissues co-expressing relatively high mRNA levels of TMPRSS2 and ACE2 include small intestine, colon, thyroid gland, kidney and breast. At protein level, only small intestine and kidney show co-expression. Interestingly, prostate expresses the highest TMPRSS2 mRNA but undetectable ACE2. These results suggest that TMPRSS2 and ACE2 are not often co-expressed in the same tissues. Notably, considerable TMPRSS2 mRNA is expressed in lung, the target tissue of SARS-CoV-2 virus, which is consistent with a promoting role of TMPRSS2 in SARS-CoV-2 infection.

As compared with ACE2 and TMPRSS2, the expression of Furin protease is much less specific at both mRNA and protein levels, though some tissues, such as liver and lung, do express much higher than the others. Regarding the 5 tissues co-expressing TMPRSS2 and ACE2, thyroid gland and kidney appear to simultaneously express high level of Furin mRNA or protein (Figure 1A, 1D, S1C and S1F).

**Expression of ACE2, TMPRSS2 and Furin in situ in tissues**

Tissues are generally comprised of multiple types of cells, therefore, the expression level of a specified gene at tissue scale may not represent for its level at certain type of cell. To address this issue, we first analysed the

protein expression of ACE2, TMPRSS2 and Furin in situ from IHC images. Tissues highly expressing ACE2 either at mRNA level or protein level were included for analysis, in addition, the putative SARS-CoV-2 target tissues proposed by previous researches irrespective of ACE2 expression level were also included. This resulted in a list of 15 tissues in total (Figure 2 and S2), which, based on the IHC intensity of ACE2, could be roughly categorised into 3 groups. The ACE2-high group contains kidney, stomach, small intestine, colon, gallbladder and testis. In this group of tissues, ACE2 was generally expressed at the apical region, facing the luminal surface, of epithelial cells (Figure 2D-E, S2B-D), which means that efficient host entry of virus could only take place from the luminal side. This rule may not be applied to testis as high level of ACE2 expression was also detected in the stromal cells (Figure 2F), which are not polarized and could be potentially accessed by virus from the blood stream. The ACE2-low group contains liver, esophagus, breast and adipose tissue, which are unlikely the direct targets of SARS-CoV-2 virus even though some of them showed high levels of mRNA expression, such as breast (Figure S2E) and adipose tissues (Figure S2F). There is a small amount of ACE2-positive cells in the interlobular region of liver tissue (Figure 2C), probably the cholanggiocytes as suggested below in scRNA analysis (Figure 4C). These cells might be potential SARS-CoV-2 targets under the condition that viruses come from the luminal side, which is normally rare, as the ACE2 protein was detected at the cell apical surface. The ACE2-median group contains lung, heart, ovary, adrenal gland and thyroid gland. For lung, the major target of SARS-CoV-2 virus, there are considerable amount of ACE2-positive cells in alveolus lumen, which morphologically resemble macrophages and represent for the majority of ACE2-positive cells in the lung tissue (Figure 2A). All of the cardiomyocytes, and a portion of stromal cells in ovary, adrenal gland and thyroid gland express ACE2 very well (Figure 2B, 2G-H, S2G), therefore are potential virus targets in the presence of viremia.

The expression of TMPRSS2 and Furin are generally also high in ACE2-high group tissues (Figure 2D-E, S2B-D) with exception for testis, where TMPRSS2 seems to be only highly enriched in the spermatids (Figure 2F). For the ACE2-low group, TMPRSS2 and Furin are also expressed in low levels (Figure S2A, S2E-F) with exception for liver, the hepatocytes in which express Furin in quite high level (Figure 2C). For the ACE2-median group, while Furin is readily detected in all the tissue cells, TMPRSS2 expression could be readily detected in lung macrophages (Figure 2A), cardiomyocytes (Figure 2B) and adrenal gland cells (Figure 2H), but not the stromal cells in ovary and thyroid gland (Figure 2G, S2G), suggesting different probabilities for them to establish efficient infection by SARS-CoV-2 virus during viremia.

Together, based on the above analysis, we propose that lung macrophages, in addition to the well-known AT2 cells, might be another direct target of SARS-CoV-2 virus. In the presence of viremia, the top vulnerable targets might be heart and adrenal gland, and then the less likely testis, ovary and thyroid gland. Other tissues are either unlikely direct targets or incompetent for establishing efficient infection due to lack of access to virus or low expression of helping proteases.

**Identification of cell types in tissues and organs by scRNA expression profiling**

To obtain comprehensive analysis of the target cells of SARS-CoV-2, we utilized the curated public database to perform scRNA profiling of the ACE2-high and -medium tissues, including lung, heart, kidney, intestinal track (ileum, rectum, colon), stomach, testis, ovary, thyroid and adrenal gland. Plus, we also included liver, the ACE2-low organ, into scRNA analysis given its important clinical implications. After quality filtering (see Material and methods), We totally obtained 122657 cells and annotated 77 cell types involving respiratory, circulatory, digestive, urinary, reproductive and endocrine systems.

The lung as the pivotal respiratory organ is one of the target organs of SARS-CoV-2. In the lung dataset, 3750 cells from an Asian donor passed stringent quality control and represented 9 cell types. Specifically, we identified alveolar type II (AT2) cells, alveolar type I (AT1) cells, ciliated and club cells, alveolar macrophages, dendritic cells, monocytes, fibroblasts, and endothelial cells. Expression of canonical cell markers for pulmonary cell types was observed in largely non-overlapping cells, including SFTPC for AT2 cells, AGER for AT1 cells,

TPPP3 for ciliated cells, SCGB3A2 for club cells, CD68 for macrophages, and VWF for endothelial cells (Figure 3A). In the heart dataset, we obtained 8148 high-quality cells involving 5 prime cell types, including cardiomyocytes, endothelial cells, fibroblasts, smooth muscle cells (SMC) and macrophages on the basis of their respective molecular features (Figure 3B).

As such, the cells population of hepatic tissues from 5 human livers were classified into ten cell types based on the expression of known markers, which was shown in Figure 3C. In addition, 23366 kidney cells from 3 donors were identified and grouped into 10 cell types. The detailed cell categories of kidney and the expression of specific cell markers were shown in Figure 3D.

For integrative analysis of human intestinal mucosa at single cell level, we pooled 14207 intestinal cells together (6167 cells from two ileum samples, 4411 cells from two colon samples and 3629 cells from two rectum samples). In total, these cells were partitioned into 7 main cell types containing enteroendocrine cells (EC), enterocytes, goblet cells, paneth cells (PC), paneth-like cells (PLC), stem cells and transient amplifying cells (TAC) (Figure 3E). Additionally, we also investigated the gastric mucosa dataset incorporating 5281 cells and finally annotated 9 cell types (Figure S3A-B).

To characterize the single-cell profiling of human reproductive organs, the testis and ovarian datasets were thoroughly analysed. In the testis datasets from adult human sorted spermatogonia, spermatocytes and spermatids, we identified 12829 cells, and classified into 5 major cell populations for downstream analysis (Figure 3F). Similarly, we exploited 27857 cells from 5 adult women ovaries, and defined 5 major cell types, including theca cells, granulosa cells, endothelial cells, SMC and immune cells (Figure 3G).

The adrenal gland and thyroid as the significant parts of the endocrine system were also included into the research. We respectively took advantage of 9809 cells of the foetal adrenal gland and 8966 cells of the thyroid to construct the single cell atlas (Figure 3H, Figure S3G). Based on the expression of specific cell markers, we found that the atlas of the adrenal gland mainly comprised epithelial cells, adrenocortical cell (AC), hepatocyte-like cell (HLC), and chromaffin cells, while the atlas of the thyroid mainly consisted of thyroid follicular cells, endothelial cells and SMC (Figure 3H, Figure S3H).

**Single cell transcriptomic profiling of ACE2, TMPRSS2 and Furin proteases in distinct cell types**

To determine the mRNA expression level of ACE2, TMPRSS2 and Furin genes in distinct tissue cells, we systematically explored the established cell atlases of different organs and tissues. We found the expression level of ACE2, TMPRSS2 and Furin genes varied significantly across the tissues and organs analyzed (Figure 4). And importantly, in certain tissues, these genes solely expressed in particular cell types. For example, the SARS-CoV-2 receptor ACE2 was mainly expressed in AT2 cells, and macrophages as well though much less, in the lung (Figure 4A), and cholangiocytes and hepatocytes in the human liver (Figure 4C), which is consistent with results of previous studies [21, 42] and confirmed our above analysis on protein expression. We further investigated the mRNA expression of TMPRSS2 and Furin proteases and confirmed that these genes were also expressed in the liver cholangiocytes, and lung macrophages and AT2 cells at the high level (Figure 4A, C). Notably, in adult human ovary, we found that merely stroma cells expressed the ACE2 and Furin gene (Figure 3G). In addition, the spermatogonia as the male reproductive cell moderately expressed the ACE2 genes as well as Furin and TMPRSS2 (Figure 4F), while the Sertoli/Leydig cells express relatively low level of TMPRSS2, which is consistent with IHC results indicated above.

Moreover, we observed that the expression of the ACE2 genes in intestine and kidney was at the top level (Figure 4D, E). But interestingly, the expression level of the TMPRSS2 and Furin genes in the kidney were not remarkable (Figure 4D), which is inconsistent with the IHC results (Figure 2D). In addition, the highly expression of the ACE2 and Furin genes were found in cardiomyocytes (Figure 4B), which fits well with the IHC result (Figure 2B). What's more, the superior expression of the ACE2 genes was also shown in the cells of fetal adrenal gland, specifically in HLC and epithelial cells, following the significant expression of the TMPRSS2 and

Furin genes (Figure 4H). By contrast, in thyroid, there was little expression of the ACE2 genes in despite of the highly expression of TMPRSS2 and Furin (Figure S3I-J), which disagrees with the IHC results that ACE2 is highly expressed in stromal cells of thyroid gland (Figure S2G). These results show that the heart and fetal adrenal gland are more likely vulnerable to the SARS-CoV-2 virus via cardiomyocytes and HLC cells, respectively.

Taken together, we comprehensively analyzed the expression of ACE2, TMPRSS2 and Furin genes in different tissue cells by feat of the scRNA-seq profiling and laid the foundation for establishing the target cells of SARS-CoV-2.

**Characterization the co-expression feature of ACE2, TMPRSS2 and Furin**

Considering the cell receptor like ACE2 together with the proteases such as TMPRSS2 and Furin are required for the SARS-CoV-2 virus to efficiently infect cells, it is imperative to characterize the co-expression patterns between ACE2 and TMPRSS2 and Furin. Accordingly, we resorted to single-cell transcriptomes to profile their co-expression patterns in the cell types identified.

The co-expression feature of these three genes was quite dominant in the intestine, specifically in enterocytes (Figure 5E), more than the other ACE2-high tissues such as kidney (Figure 5D), testis (Figure 5F) and stomach (Figure S3F). For example, as shown in Figure 5D, though the cells in the kidney expressed ACE2, TMPRSS2 and Furin at moderate to high level, there was only a small fraction of co-expression cells. The ACE2-low liver tissue displayed an interesting expression pattern, while the co-expression of Furin and TMPRSS2 in the hepatocytes and cholangiocytes were remarkable, their co-expression with ACE2 were much less (Figure 5C), arguing against liver as a primary SARS-CoV-2 target.

In the ACE2-medium tissues, we found the AT2 cells, and macrophages as well, in the lung possessed the co-expression feature (Figure 5A), which provided the hard evidence that SARS-CoV-2 posed the serious threat to the lung. Moreover, we observed a significant co-expression of the ACE2 gene with TMPRSS2 and Furin in the epithelial cells and HLC of the fetal adrenal gland (Figure 5H), manifesting that the fetal adrenal gland may be a target of SARS-CoV-2. Furthermore, in consistence with the results above, a portion of cardiomyocytes simultaneously expressed ACE2 and Furin (Figure 5B). However, few cells co-expressed ACE2, TMPRSS2 and Furin simultaneously in the ovary (Figure 5G) and thyroid gland (Figure S3K-L).

**DISCUSSION**

The identification of lung macrophages and adrenal gland stromal cells as the SARS-CoV-2 targets might be much informative for clinical practises and translational researches, because the COVID-19 disease frequently proceeded to severe or very severe stage in a short period [1], which suggests systemic conditions occurred probably due to the deregulated immune and endocrine systems. Whereas, macrophages are critical inflammatory cells that were linked to the cytokine storm [43, 44], a severe condition leading to patient death; meanwhile, adrenal gland, via producing multiple hormones such as glucocorticoid, plays a central role in the endocrine homeostasis [45]. Therefore, it's conceivable that their infection by SARS-CoV-2 may be accountable for the rapid progression and severe conditions of COVID-19 disease. Additionally, stromal cells in reproductive system (ovary and testis) and thyroid gland were also identified as potential target cells under the condition of viremia, suggesting potential injuries in these tissues. Actually, a recent study reported a significant change in certain male sex hormones in COVID-19 male patients [46], which is consistent with the notion that testis is potentially targeted by SARS-CoV-2.

Previous analysis based solely on the mRNA expression of ACE2 suggested multiple tissue cells as potential targets of the novel coronavirus SARS-CoV-2, including cells from almost every important human system. However, the COVID-19 patients primarily displayed symptoms from respiratory systems, where ACE2 is expressed in a small portion of cells. Even for severely ill patients, the injuries or symptoms in the ACE2-high organs such as kidney and intestinal tract are relatively uncommon, with a rate of 1%-4.3% for acute kidney

injury [1, 25], and a rate of 3.5%-5.8% for intestinal symptoms [1, 47]. Instead, the injuries in ACE2-median organs such as heart are more frequent (12%-19%) [1, 47]. This obvious discrepancy suggests that mechanisms other than ACE2 expression level also play important roles in establishing efficient and successful infection. Based on our above analysis by pscRNA expression profiling, we propose that three more factors, in addition to the mRNA level, should be taken into account in predicting the vulnerability of a specified target tissue/organ.

First, the protein information of expression level, subcellular localization may influence virus infection. As shown above, the mRNA level is not often corresponding to protein level, such as in kidney and adipose tissue (Figure 1), therefore, it's necessary to not only analyse mRNA expression, but also detect protein expression in situ. Moreover, membrane proteins such as ACE2 could be expressed either all around the surface of non-polarized stromal cells such as Leydig cells in testis (Figure 2F and 3F), or specifically on the apical region of polarized epithelial cells such as the enterocytes in intestinal tracts (Figure 2E). This means much for virus infection as it determines how the viruses may get access to their target cells and enter. For the polarized cells, virus could only successfully infect cells from the luminal side, where ACE2 is expressed on apical surface but not the basal-lateral surfaces. While for the non-polarized stromal cells, virus may readily come to see them from the blood stream.

Second, the co-expression of infection co-factors determines the efficiency of successful infection. As for SARS-CoV-2, TMPRSS2 and Furin were demonstrated to be important proteases that cleave the S protein to promote host entry [13, 14, 16]. Threrefore, their co-expression with ACE2, the cellular receptor for SARS-CoV-2, may dictate the vulnerability of the target tissues. Actually, we found that some ACE2-high cells, such as stromal cells in testis and ovary, express TMPRSS2 at quite low levels (Figure 2F-G), suggesting that they may not be SARS-CoV-2 targets as susceptible as those co-expressing both ACE2 and TMPRSS2/Furin proteases, such as heart though cardiomyocytes express relatively lower level of ACE2. It's conceivable that cells highly co-expressing ACE2, TMPRSS2 and Furin proteases, such as lung macrophages and stromal cells in adrenal gland, would be readily vulnerable to SARS-CoV-2 attack in the presence of viruses.

Third, the feasible routes whereby viruses get access to their target cells are also accountable for clinical manifestations. In theory, there are two major routes for virus transmission: 1) directly entering the luminal tracks via open entries of the body. The potentially affected tissues/organs include those from the respiratory system, digestive system and urinary tract, among which the respiratory system is much easier than the rest two to be infected as it's almost a completely open system while the rest two are gated by multiple ways. This may explain the prominent symptoms in respiratory system but not in the digestive and urinary systems despite high level of co-expression of ACE2, TMPRSS2 and Furin in epithelial cells lining along the tracts of the later two systems; 2) transmitting via blood stream to the entire body. This may theoretically affect all the internal organs with stromal cells expressing ACE2, with exception for those polarized cells in which the ACE2 protein is only expressed in the apical surface unreachable by the viruses from viremia. The target tissue cells affected by this route may include cardiomyocytes, stromal cells in adrenal gland, Leydig cells in testis, and stromal cells in ovary and thyroid gland. Among them, only the former two, but not the later three, are more likely the true or susceptible targets of SARS-CoV-2 when considering the co-expression of helping proteases with ACE2. It should be noted that the precondition for this route is viremia, which, however to our best knowledge, was not clearly documented in COVID-19 patients up to date. Nevertheless, frequent heart injuries in COVID-19 patients [1, 48] are consistent with the presence of occasional viremia. Under such circumstances, adrenal gland may be another vulnerable target of SARS-CoV-2, which, to our best knowledge, is identified for the first time in this study.

In summary, we propose the pscRNA profiling a feasible way for gene expression analysis at both protein and mRNA levels. And through systemic analysis of 36 human tissues/organs by pscRNA profiling of ACE2, TMPRSS2 and Furin proteases, we propose a rank list of tissue cells potentially vulnerable to SARS-CoV-2 attack. For initial infection, ACE2-expression cells, with the co-expression of TMPRSS2 and Furin as a plus, in respiratory track are the primary targets. These cells include the known lung AT2 cells, and macrophages in

this study, and also the nasal epithelial cells as reported recently [19]. And the likelihood for epithelial cells in digestive and urinary system as the primary target are low. During the period of viremia if there was, the top internal organ targets would be cardiomyocytes, and stromal cells in adrenal gland, both of them express all three ACE2, TMPRSS2 and Furin proteases; the descent targets may be Leydig cells in testis, and stromal cells in ovary and thyroid gland, these cells are un-polarized and ACE2-positve, but don't show ideal co-expression of TMPRSS2 or Furin proteases.

## DATA AVAILABILITY

Availability of supporting data: GSE122960 (http://www.ncbi.nlm.nih.gov/geo/query/acc.cgi?acc=GSE122960), GSE109816 (http://www.ncbi.nlm.nih.gov/geo/query/acc.cgi?acc=GSE109816), GSE131685 (http://www.ncbi.nlm.nih.gov/geo/query/acc.cgi?acc=GSE131685), GSE125970 (http://www.ncbi.nlm.nih.gov/geo/query/acc.cgi?acc=GSE125970), GSE134520 (http://www.ncbi.nlm.nih.gov/geo/query/acc.cgi?acc=GSE134520), GSE109037 (http://www.ncbi.nlm.nih.gov/geo/query/acc.cgi?acc=GSE109037), GSE134355 (http://www.ncbi.nlm.nih.gov/geo/query/acc.cgi?acc=GSE134355), GSE118127 (http://www.ncbi.nlm.nih.gov/geo/query/acc.cgi?acc=GSE118127).

## ACKNOWLEDGEMENT

We thank Dr. Yan Zhang from the institute of biotechnology, Beijing, for assisting database analysis.

## FUNDING

This work was supported by the National Key Research & Development Program of China [2018YFA0900804 to Y.Z., 2019YFA09003801 to Q.S.] and the National Natural Science Foundation of China [31970685 to Q.S., 31770975 to X.W.].

## CONFLICT OF INTEREST

No

## REFERENCES

[1] Guan WJ, Ni ZY, Hu Y, Liang WH, Ou CQ, He JX, et al. Clinical Characteristics of Coronavirus Disease 2019 in China. N Engl J Med 2020;10.1056/NEJMoa2002032.
[2] Novel Coronavirus Pneumonia Emergency Response Epidemiology T. [The epidemiological characteristics of an outbreak of 2019 novel coronavirus diseases (COVID-19) in China]. Zhonghua Liu Xing Bing Xue Za Zhi. 2020;41:145-51.
[3] Zhu N, Zhang D, Wang W, Li X, Yang B, Song J, et al. A Novel Coronavirus from Patients with Pneumonia in China, 2019. N Engl J Med 2020;382:727-33.
[4] Tang X, Wu C, Li X, Song Y, Yao X, Wu X, et al. On the origin and continuing evolution of SARS-CoV-2. National Science Review 2020;10.1093/nsr/nwaa036.
[5] Wu F, Zhao S, Yu B, Chen Y-M, Wang W, Song Z-G, et al. A new coronavirus associated with human respiratory disease in China. Nature 2020;10.1038/s41586-020-2008-3.
[6] Xu X, Chen P, Wang J, Feng J, Zhou H, Li X, et al. Evolution of the novel coronavirus from the ongoing Wuhan outbreak and modeling of its spike protein for risk of human transmission. Sci China Life Sci 2020;10.1007/s11427-020-1637-5.
[7] Zhou P, Yang XL, Wang XG, Hu B, Zhang L, Zhang W, et al. A pneumonia outbreak associated with a new coronavirus of probable bat origin. Nature 2020;579:270-3.

[8] Zhu N, Zhang D, Wang W, Li X, Yang B, Song J, et al. A Novel Coronavirus from Patients with Pneumonia in China, 2019. N Engl J Med 2020;382:727-33.
[9] WHO. Coronavirus disease (COVID-2019) situation report-69. Situation reports 2020;20200318-sitrep-69-covid-19:https://www.who.int/emergencies/diseases/novel-coronavirus-2019/situation-reports.
[10] Li F. Structure, Function, and Evolution of Coronavirus Spike Proteins. Annu Rev Virol 2016;3:237-61.
[11] Millet JK, Whittaker GR. Host cell proteases: Critical determinants of coronavirus tropism and pathogenesis. Virus Res 2015;202:120-34.
[12] Li W, Moore MJ, Vasilieva N, Sui J, Wong SK, Berne MA, et al. Angiotensin-converting enzyme 2 is a functional receptor for the SARS coronavirus. Nature 2003;426:450-4.
[13] Walls AC, Park YJ, Tortorici MA, Wall A, McGuire AT, Veesler D. Structure, Function, and Antigenicity of the SARS-CoV-2 Spike Glycoprotein. Cell 2020;10.1016/j.cell.2020.02.058.
[14] Hoffmann M, Kleine-Weber H, Schroeder S, Kruger N, Herrler T, Erichsen S, et al. SARS-CoV-2 Cell Entry Depends on ACE2 and TMPRSS2 and Is Blocked by a Clinically Proven Protease Inhibitor. Cell 2020;10.1016/j.cell.2020.02.052.
[15] Wrapp D, Wang N, Corbett KS, Goldsmith JA, Hsieh CL, Abiona O, et al. Cryo-EM structure of the 2019-nCoV spike in the prefusion conformation. Science 2020;367:1260-3.
[16] Meng T, Cao H, Zhang H, Kang Z, Xu D, Gong H, et al. The insert sequence in SARS-CoV-2 enhances spike protein cleavage by TMPRSS. bioRxiv 2020;10.1101/2020.02.08.926006:2020.02.08.926006.
[17] Li X, Duan G, Zhang W, Shi J, Chen J, Chen S, et al. A furin cleavage site was discovered in the S protein of the Wuhan 2019 novel coronavirus. Chinese Journal of Bioinformatics 2020;10.12074/202002.0000.
[18] Zhao Y, Zhao Z, Wang Y, Zhou Y, Ma Y, Zuo W. Single-cell RNA expression profiling of ACE2, the putative receptor of Wuhan 2019-nCov. bioRxiv 2020;10.1101/2020.01.26.919985:2020.01.26.919985.
[19] WU C, Zheng S, Chen Y, Zheng M. Single-cell RNA expression profiling of ACE2, the putative receptor of Wuhan 2019-nCoV, in the nasal tissue. medRxiv 2020;10.1101/2020.02.11.20022228:2020.02.11.20022228.
[20] Zhang H, Kang Z, Gong H, Xu D, Wang J, Li Z, et al. The digestive system is a potential route of 2019-nCov infection: a bioinformatics analysis based on single-cell transcriptomes. bioRxiv 2020;10.1101/2020.01.30.927806:2020.01.30.927806.
[21] Chai X, Hu L, Zhang Y, Han W, Lu Z, Ke A, et al. Specific ACE2 Expression in Cholangiocytes May Cause Liver Damage After 2019-nCoV Infection. bioRxiv 2020;10.1101/2020.02.03.931766.
[22] Xin Zou KC, Jiawei Zou, Peiyi Han, Jie Hao, Zeguang Han. Single-cell RNA-seq data analysis on the receptor ACE2 expression reveals the potential risk of different human organs vulnerable to 2019-nCoV infection. Front. Med.;10.1007/s11684-020-0754-0:0-.
[23] Lin W, Hu L, Zhang Y, Ooi JD, Meng T, Jin P, et al. Single-cell Analysis of ACE2 Expression in Human Kidneys and Bladders Reveals a Potential Route of 2019-nCoV Infection. bioRxiv 2020;10.1101/2020.02.08.939892:2020.02.08.939892.
[24] Zhengpin W, Xiaojiang X. scRNA-seq Profiling of Human Testes Reveals the Presence of ACE2 Receptor, a Target for SARS-CoV-2 Infection, in Spermatogonia, Leydig and Sertoli Cells. Preprints 2020; doi: 10.20944/preprints202002.0299.v1.
[25] Wang L, Li X, Chen H, Yan S, Li Y, Li D, et al. SARS-CoV-2 infection does not significantly cause acute renal injury: an analysis of 116 hospitalized patients with COVID-19 in a single hospital, Wuhan, China. SSRN3541116 2020.
[26] Reyfman PA, Walter JM, Joshi N, Anekalla KR, McQuattie-Pimentel AC, Chiu S, et al. Single-Cell Transcriptomic Analysis of Human Lung Provides Insights into the Pathobiology of Pulmonary Fibrosis. Am. J. Respir. Crit. Care Med. 2019;199:1517-36.
[27] Wang L, Yu P, Zhou B, Song J, Li Z, Zhang M, et al. Single-cell reconstruction of the adult human heart during heart failure and recovery reveals the cellular landscape underlying cardiac function. Nat. Cell Biol. 2020;22:108-19.
[28] Liao J, Yu Z, Chen Y, Bao M, Zou C, Zhang H, et al. Single-cell RNA sequencing of human kidney. Scientific Data 2020;7.
[29] Wang Y, Song W, Wang J, Wang T, Xiong X, Qi Z, et al. Single-cell transcriptome analysis reveals differential nutrient absorption functions in human intestine. J. Exp. Med. 2020;217.

[30] Zhang P, Yang M, Zhang Y, Xiao S, Lai X, Tan A, et al. Dissecting the Single-Cell Transcriptome Network Underlying Gastric Premalignant Lesions and Early Gastric Cancer. Cell Rep 2019;27:1934-47.e5.
[31] Hermann BP, Cheng K, Singh A, Roa-De La Cruz L, Mutoji KN, Chen IC, et al. The Mammalian Spermatogenesis Single-Cell Transcriptome, from Spermatogonial Stem Cells to Spermatids. Cell Rep 2018;25:1650-67.e8.
[32] Han X, Zhou Z, Fei L, Sun H, Wang R, Chen Y, et al. Construction of a human cell landscape at single-cell level. Nature 2020;10.1038/s41586-020-2157-4.
[33] Fan X, Bialecka M, Moustakas I, Lam E, Torrens-Juaneda V, Borggreven NV, et al. Single-cell reconstruction of follicular remodeling in the human adult ovary. Nat Commun 2019;10.
[34] MacParland SA, Liu JC, Ma X-Z, Innes BT, Bartczak AM, Gage BK, et al. Single cell RNA sequencing of human liver reveals distinct intrahepatic macrophage populations. Nat Commun 2018;9.
[35] Uhlen M, Fagerberg L, Hallstrom BM, Lindskog C, Oksvold P, Mardinoglu A, et al. Proteomics. Tissue-based map of the human proteome. Science 2015;347:1260419.
[36] Carithers LJ, Moore HM. The Genotype-Tissue Expression (GTEx) Project. Biopreserv Biobank 2015;13:307-8.
[37] Thul PJ, Akesson L, Wiking M, Mahdessian D, Geladaki A, Ait Blal H, et al. A subcellular map of the human proteome. Science 2017;356.
[38] Stuart T, Butler A, Hoffman P, Hafemeister C, Papalexi E, Mauck WM, et al. Comprehensive Integration of Single-Cell Data. Cell 2019;177:1888-902.e21.
[39] Korsunsky I, Millard N, Fan J, Slowikowski K, Zhang F, Wei K, et al. Fast, sensitive and accurate integration of single-cell data with Harmony. Nat. Methods 2019;16:1289-96.
[40] Zhang X, Lan Y, Xu J, Quan F, Zhao E, Deng C, et al. CellMarker: a manually curated resource of cell markers in human and mouse. Nucleic Acids Res. 2019;47:D721-D8.
[41] Yu G, Wang LG, Han Y, He QY. clusterProfiler: an R package for comparing biological themes among gene clusters. OMICS 2012;16:284-7.
[42] Zhao Y, Zhao Z, Wang Y, Zhou Y, Ma Y, Zuo W. Single-cell RNA expression profiling of ACE2, the putative receptor of Wuhan 2019-nCov. bioRxiv 2020;10.1101/2020.01.26.919985.
[43] Channappanavar R, Fehr AR, Vijay R, Mack M, Zhao J, Meyerholz DK, et al. Dysregulated Type I Interferon and Inflammatory Monocyte-Macrophage Responses Cause Lethal Pneumonia in SARS-CoV-Infected Mice. Cell Host Microbe 2016;19:181-93.
[44] Channappanavar R, Perlman S. Pathogenic human coronavirus infections: causes and consequences of cytokine storm and immunopathology. Semin Immunopathol 2017;39:529-39.
[45] Berger I, Werdermann M, Bornstein SR, Steenblock C. The adrenal gland in stress - Adaptation on a cellular level. J Steroid Biochem Mol Biol 2019;190:198-206.
[46] Ma L, Xie W, Li D, Shi L, Mao Y, Xiong Y, et al. Effect of SARS-CoV-2 infection upon male gonadal function: A single center-based study. medRxiv 2020;10.1101/2020.03.21.20037267:2020.03.21.20037267.
[47] Special Expert Group for Control of the Epidemic of Novel Coronavirus Pneumonia of the Chinese Preventive Medicine A. [An update on the epidemiological characteristics of novel coronavirus pneumoniaCOVID-19]. Zhonghua Liu Xing Bing Xue Za Zhi 2020;41:139-44.
[48] Zhou B, She J, Wang Y, Ma X. The Clinical Characteristics of Myocardial Injury in Severe and Very Severe Patients with 2019 Novel Coronavirus Disease (2/16/2020). SSRN 2020;10.2139/ssrn.3539668.

## FIGURES LEGENDS

**Figure 1. Tissue distribution of ACE2, TMPRSS2 and Furin proteases**. (A) the anatomogram of the expression of ACE2, TMPRSS2, and ACE2 in male and female human tissues, respectively. The colour strength is corresponding to the gene expression level. (B-D) the mRNA expression level and protein expression score of ACE2 (B), TMPRSS2 (C) and Furin (D) in the manifold tissues and organs. N: negative; L: low expression shown in short blue column; M: median expression shown in pink column; H: high expression shown in long red column. TPM: transcripts per million; pTPM: all TPM values per sample scaled to a sum of 1 million TPM.

**Figure 2. Protein expression of ACE2, TMPRSS2 and Furin in situ in tissues**. (A-H) the IHC images for the protein expression of ACE2, TMPRSS2 and Furin in the indicated tissues/organs, respectively. F. adrenal gland: fetal adrenal gland. Scale bars: 200 μm for core images, 20 μm for zoom in images. Arrows indicate the positive IHC signals.

**Figure 3. Single cell profiling of the cell types in tissues and organs**. The UMAP plots in the left show single cell transcriptomic profiling of the cell types from the indicated tissues/organs. The dot plots or heatmaps in the right represent the expression of canonical marker genes of each cell types. AT2: alveolar type II, AT1: alveolar type I, SMC: smooth muscle cells, NK: natural killer, CTC: convoluted tubule cells, TC: tubule cells, STC: straight tubule cells, PEC: parietal epithelial cells, TC: tubule cells, DPC: duct principal cells, DIC: distal tubule cells, EC: enteroendocrine cells, PC: paneth cells, PLC: paneth-like cells, TAC: transient amplifying cells, AC: adrenocortical cell, HLC: hepatocyte-like cell, F. adrenal gland: fetal adrenal gland.

**Figure 4. Single cell transcriptomic profiling of ACE2, TMPRSS2 and Furin proteases in distinct cell types.** The UMAP plots (left panel) and violin plots (right panel) show the mRNA expression of ACE2, TMPRSS2 and Furin genes in different tissue cells from the indicated tissues/organs. AT2: alveolar type II, AT1: alveolar type I, SMC: smooth muscle cells, NK: natural killer, CTC: convoluted tubule cells, TC: tubule cells, STC: straight tubule cells, PEC: parietal epithelial cells, TC: tubule cells, DPC: duct principal cells, DIC: distal tubule cells, EC: enteroendocrine cells, PC: paneth cells, PLC: paneth-like cells, TAC: transient amplifying cells, HLC: hepatocyte-like cell, AC: adrenocortical cell, F. adrenal gland: fetal adrenal gland.

**Figure 5. Characterizing the co-expression patterns of ACE2, TMPRSS2 and Furin at single cell level.** The UMAP plots (left panels) show the co-expression of two individual genes of Furin, TMPRSS2, and ACE2 in the indicated tissues/organs. Scatter plots (right panels) illustrate the expression correlation of two individual genes of Furin, TMPRSS2, and ACE2 in the AT2 cells and macrophages of lung (A), the cardiomyocytes of heart (B), the hepatocytes and cholangiocytes of liver (C), the proximal tubule cells of kidney (D), the enterocyte of intestinal tract (E), the spermatogonia and Sertoli/Leydig cells in testis (F), the stroma cells and granulosa cells in ovary (G), the epithelial cell and HLC in fetal adrenal gland (H).

## SUPPLEMENTAL FIGURES LEGENDS

**Figure S1. Tissue distribution of ACE2, TMPRSS2 and Furin proteases.** (A-C) The normalized mRNA expression of ACE2, TMPRSS2 and Furin in 61 human tissues and organs. (D-F) The protein expression scores for ACE2, TMPRSS2 and Furin in 44 human tissues and organs.

**Figure S2. Protein expression of ACE2, TMPRSS2 and Furin in situ in tissues**. The IHC images for ACE2, TMPRSS2 and Furin in tissues of esophagus (A), stomach (B), colon (C), gallbladder (D), breast (E), adipose tissue (F), and thyroid gland (G). Scale bars: 200 μm for core images, 20 μm for zoom in images. Arrows indicate the positive IHC signals.

**Figure S3. Single cell transcriptomic profiling of ACE2, TMPRSS2 and Furin expression in the gastric tissue and thyroid gland**. (A) The tSNE plot showing different cell types in the stomach. (B) The dot plot showing the expression level of specific cell markers in each cell types of the gastric tissue. (C) The tSNE plot revealing the expression distribution of Furin, TMPRSS2 and ACE2 in the stomach. (D) The violin plot showing the expression level of Furin, TMPRSS2 and ACE2 in different cell types of the stomach. (E-L) The characterization of the co-expression feature of ACE2, Furin and TMPRSS2 in the stomach. (G) The UMAP plot representing different cell types in the thyroid gland. (H) The dot plot showing the expression level of known cell markers in each cell types of the thyroid gland. (I) The UMAP plot illustrating the expression distribution of Furin, TMPRSS2 and ACE2 in the thyroid gland. (J) The violin plot showing the expression level of Furin, TMPRSS2 and ACE2 in different cell types of the thyroid gland. (K-L) The characterization the co-expression feature of ACE2, Furin and TMPRSS2 in the thyroid gland.

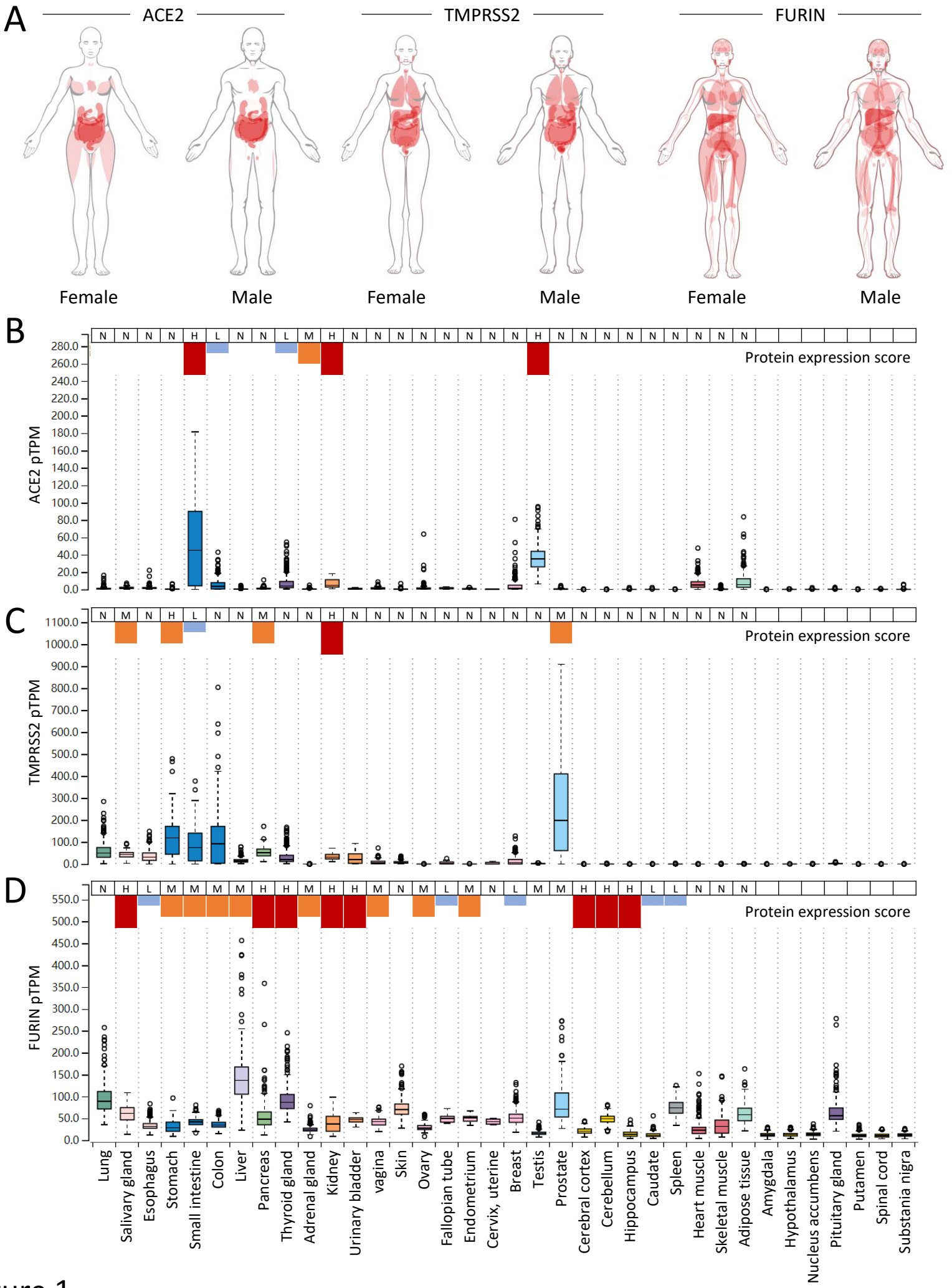
A
ACE2
TMPRSS2
FURIN
Female
Male
Female
Male
Female
Male
B
Protein expression score
ACE2 pTPM
C
Protein expression score
TMPRSS2 pTPM
D
Protein expression score
FURIN pTPM
Lung
Salivary gland
Esophagus
Stomach
Small intestine
Colon
Liver
Pancreas
Thyroid gland
Adrenal gland
Kidney
Urinary bladder
vagina
Skin
Ovary
Fallopian tube
Endometrium
Cervix, uterine
Breast
Testis
Prostate
Cerebral cortex
Cerebellum
Hippocampus
Caudate
Spleen
Heart muscle
Skeletal muscle
Adipose tissue
Amygdala
Hypothalamus
Nucleus accumbens
Pituitary gland
Putamen
Spinal cord
Substania nigra

Figure 1

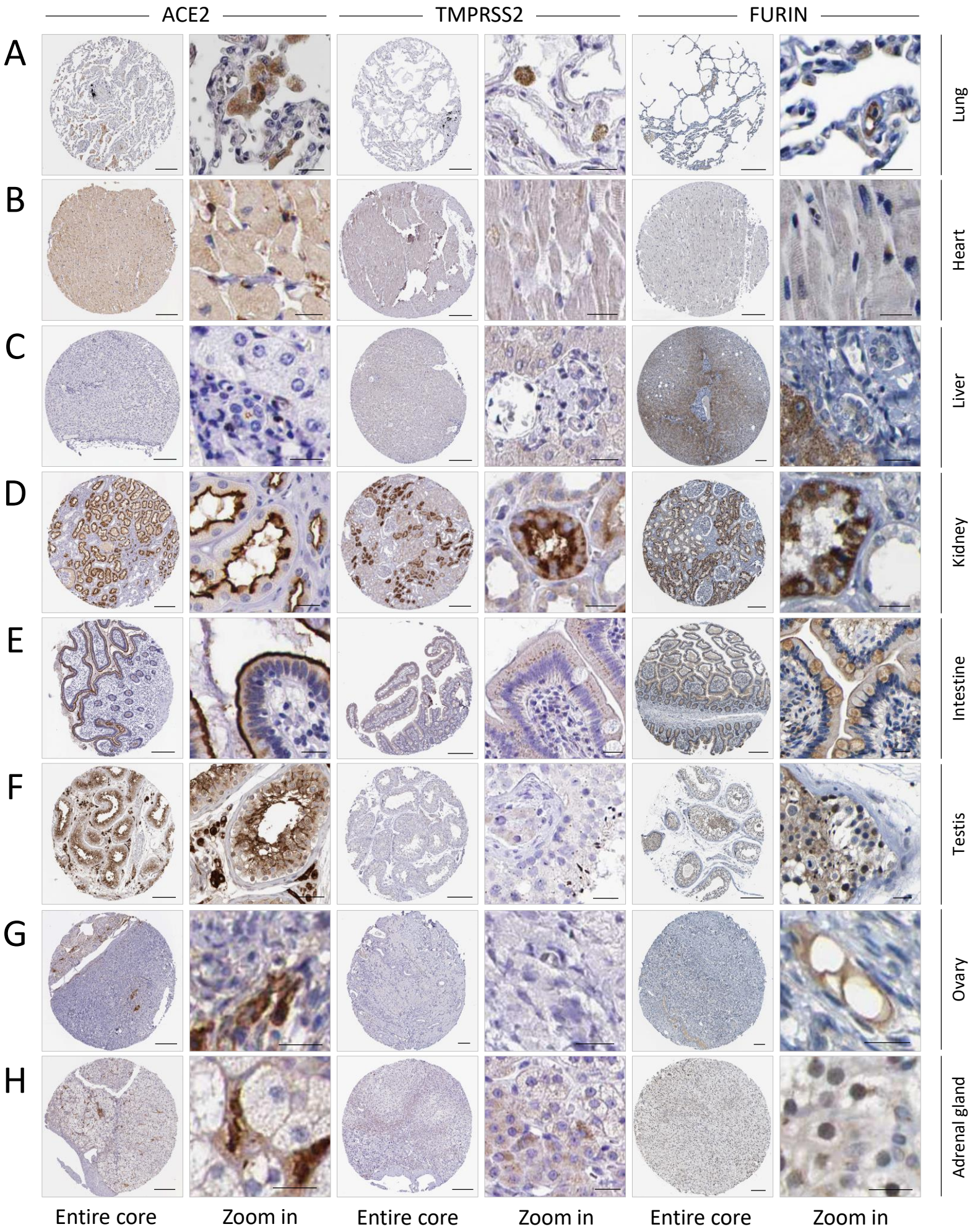
ACE2
TMPRSS2
FURIN
A
B
C
D
E
F
G
H
Lung
Heart
Liver
Kidney
Intestine
Testis
Ovary
Adrenal gland
Entire core
Zoom in
Entire core
Zoom in
Entire core
Zoom in

Figure 2

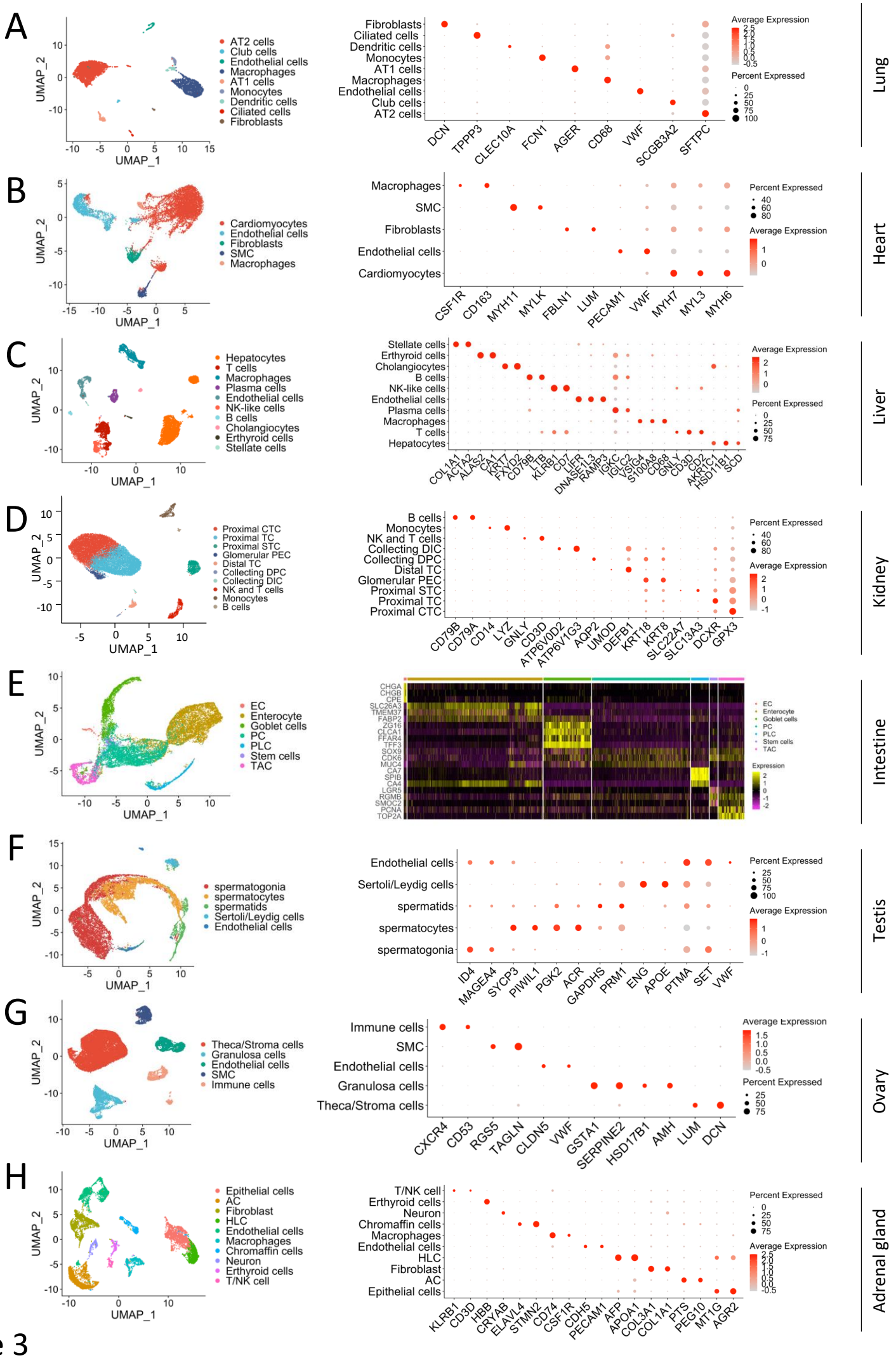
A
UMAP_2
UMAP_1
AT2 cells
Club cells
Endothelial cells
Macrophages
AT1 cells
Monocytes
Dendritic cells
Ciliated cells
Fibroblasts
Fibroblasts
Ciliated cells
Dendritic cells
Monocytes
AT1 cells
Macrophages
Endothelial cells
Club cells
AT2 cells
DCN
TPPP3
CLEC10A
FCN1
AGER
CD68
VWF
SCGB3A2
SFTPC
Average Expression
Percent Expressed
Lung
B
Cardiomyocytes
Endothelial cells
Fibroblasts
SMC
Macrophages
Macrophages
SMC
Fibroblasts
Endothelial cells
Cardiomyocytes
CSF1R
CD163
MYH11
MYLK
FBLN1
LUM
PECAM1
VWF
MYH7
MYL3
MYH6
Percent Expressed
Average Expression
Heart
C
Hepatocytes
T cells
Macrophages
Plasma cells
Endothelial cells
NK-like cells
B cells
Cholangiocytes
Erthyroid cells
Stellate cells
Stellate cells
Erthyroid cells
Cholangiocytes
B cells
NK-like cells
Endothelial cells
Plasma cells
Macrophages
T cells
Hepatocytes
COL1A1
ACTA2
ALAS2
CA1
KRT7
FXYD2
CD79B
LTB
KLRB1
CD7
LIFR
DNASE1L3
RAMP3
IGKC
IGLC2
VSIG4
S100A8
CD68
GNLY
CD3D
CD2
AKR1C1
HSD11B1
SCD
Average Expression
Percent Expressed
Liver
D
Proximal CTC
Proximal TC
Proximal STC
Glomerular PEC
Distal TC
Collecting DPC
Collecting DIC
NK and T cells
Monocytes
B cells
B cells
Monocytes
NK and T cells
Collecting DIC
Collecting DPC
Distal TC
Glomerular PEC
Proximal STC
Proximal TC
Proximal CTC
CD79B
CD79A
CD14
LYZ
GNLY
CD3D
ATP6V0D2
ATP6V1G3
AQP2
UMOD
DEFB1
KRT18
KRT8
SLC22A7
SLC13A3
DCXR
GPX3
Percent Expressed
Average Expression
Kidney
E
EC
Enterocyte
Goblet cells
PC
PLC
Stem cells
TAC
CHGA
CHGB
CPE
SLC26A3
TMEM37
FABP2
ZG16
CLCA1
FFAR4
TFF3
SOX9
CDK6
MUC4
CA7
SPIB
CA4
LGR5
RGMB
SMOC2
PCNA
TOP2A
Expression
Intestine
F
spermatogonia
spermatocytes
spermatids
Sertoli/Leydig cells
Endothelial cells
Endothelial cells
Sertoli/Leydig cells
spermatids
spermatocytes
spermatogonia
ID4
MAGEA4
SYCP3
PIWIL1
PGK2
ACR
GAPDHS
PRM1
ENG
APOE
PTMA
SET
VWF
Percent Expressed
Average Expression
Testis
G
Theca/Stroma cells
Granulosa cells
Endothelial cells
SMC
Immune cells
Immune cells
SMC
Endothelial cells
Granulosa cells
Theca/Stroma cells
CXCR4
CD53
RGS5
TAGLN
CLDN5
VWF
GSTA1
SERPINE2
HSD17B1
AMH
LUM
DCN
Average Expression
Percent Expressed
Ovary
H
Epithelial cells
AC
Fibroblast
HLC
Endothelial cells
Macrophages
Chromaffin cells
Neuron
Erthyroid cells
T/NK cell
T/NK cell
Erthyroid cells
Neuron
Chromaffin cells
Macrophages
Endothelial cells
HLC
Fibroblast
AC
Epithelial cells
KLRB1
CD3D
HBB
CRYAB
ELAVL4
STMN2
CD74
CSF1R
CDH5
PECAM1
AFP
APOA1
COL3A1
COL1A1
PTS
PEG10
MT1G
AGR2
Percent Expressed
Average Expression
Adrenal gland

Figure 3

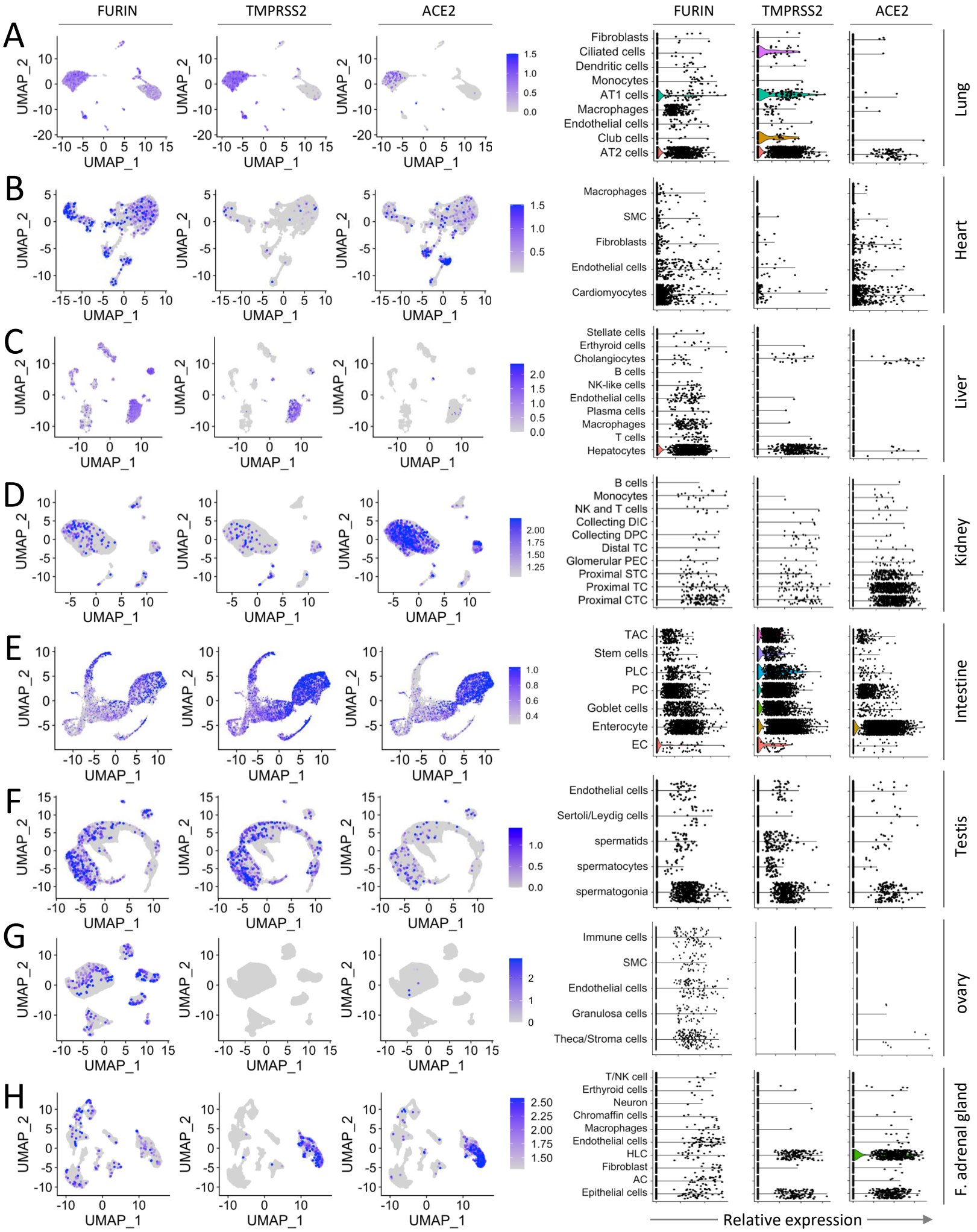
FURIN
TMPRSS2
ACE2
A
B
C
D
E
F
G
H
UMAP_1
UMAP_2
Fibroblasts
Ciliated cells
Dendritic cells
Monocytes
AT1 cells
Macrophages
Endothelial cells
Club cells
AT2 cells
Lung
Macrophages
SMC
Fibroblasts
Endothelial cells
Cardiomyocytes
Heart
Stellate cells
Erthyroid cells
Cholangiocytes
B cells
NK-like cells
Endothelial cells
Plasma cells
Macrophages
T cells
Hepatocytes
Liver
B cells
Monocytes
NK and T cells
Collecting DIC
Collecting DPC
Distal TC
Glomerular PEC
Proximal STC
Proximal TC
Proximal CTC
Kidney
TAC
Stem cells
PLC
PC
Goblet cells
Enterocyte
EC
Intestine
Endothelial cells
Sertoli/Leydig cells
spermatids
spermatocytes
spermatogonia
Testis
Immune cells
SMC
Endothelial cells
Granulosa cells
Theca/Stroma cells
ovary
T/NK cell
Erthyroid cells
Neuron
Chromaffin cells
Macrophages
Endothelial cells
HLC
Fibroblast
AC
Epithelial cells
F. adrenal gland
Relative expression

Figure 4

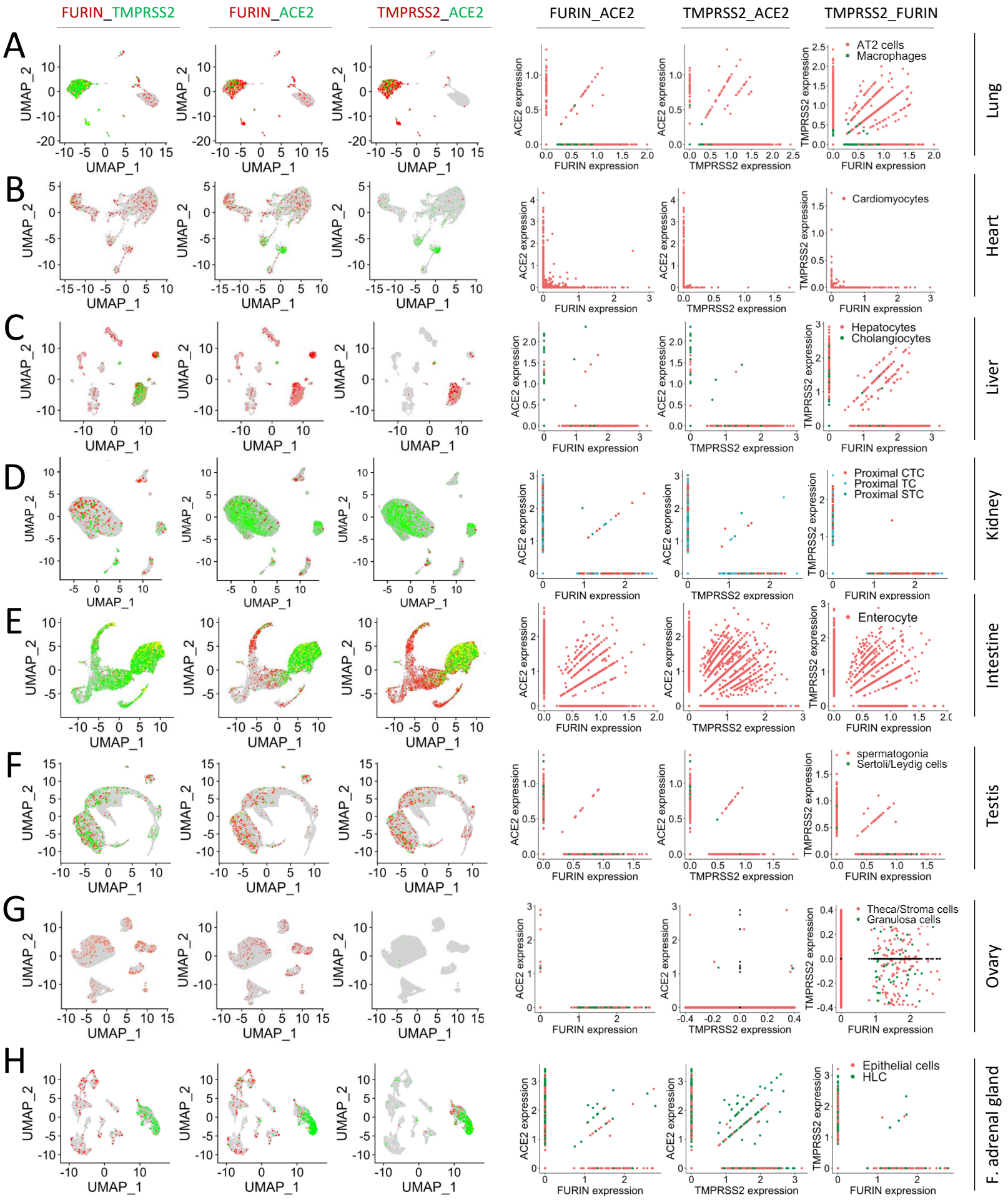
FURIN_TMPRSS2
FURIN_ACE2
TMPRSS2_ACE2
FURIN_ACE2
TMPRSS2_ACE2
TMPRSS2_FURIN
A
B
C
D
E
F
G
H
UMAP_1
UMAP_2
ACE2 expression
FURIN expression
TMPRSS2 expression
TMPRSS2 expression
AT2 cells
Macrophages
Lung
Cardiomyocytes
Heart
Hepatocytes
Cholangiocytes
Liver
Proximal CTC
Proximal TC
Proximal STC
Kidney
Enterocyte
Intestine
spermatogonia
Sertoli/Leydig cells
Testis
Theca/Stroma cells
Granulosa cells
Ovary
Epithelial cells
HLC
F. adrenal gland

Figure 5

# Supplemental figures

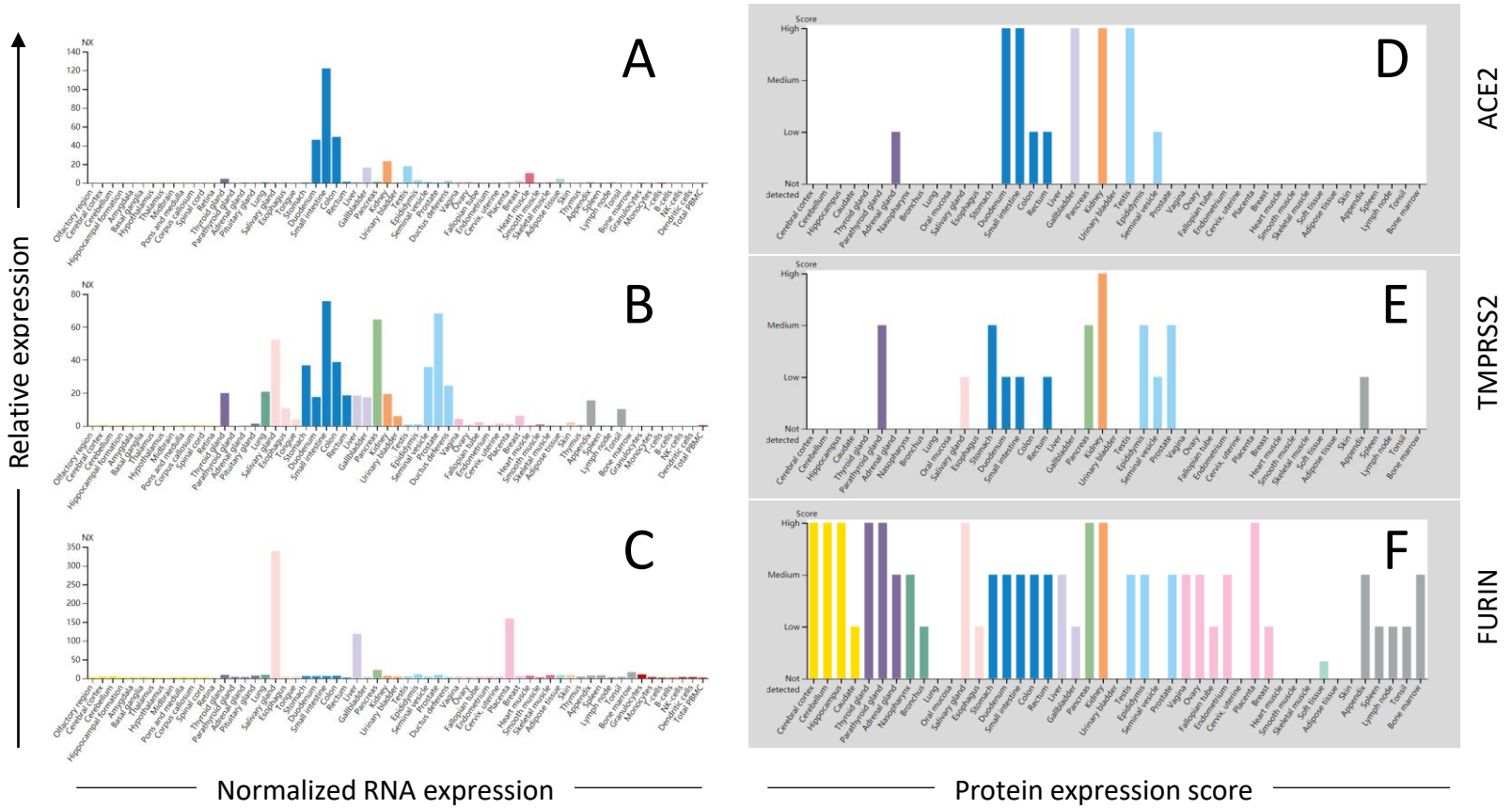


Figure S1

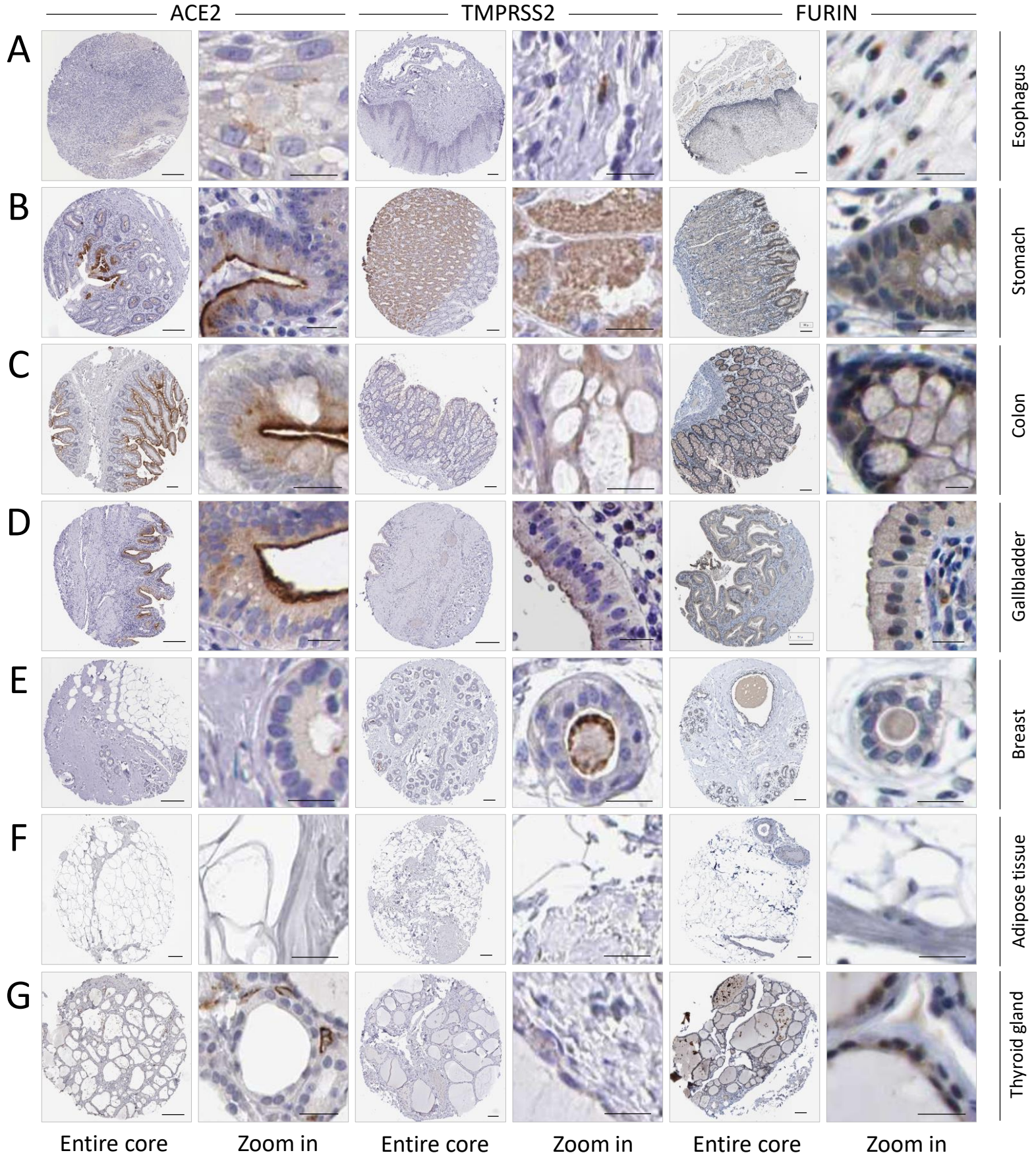
ACE2
TMPRSS2
FURIN
A
B
C
D
E
F
G
Esophagus
Stomach
Colon
Gallbladder
Breast
Adipose tissue
Thyroid gland
Entire core
Zoom in
Entire core
Zoom in
Entire core
Zoom in

Figure S2

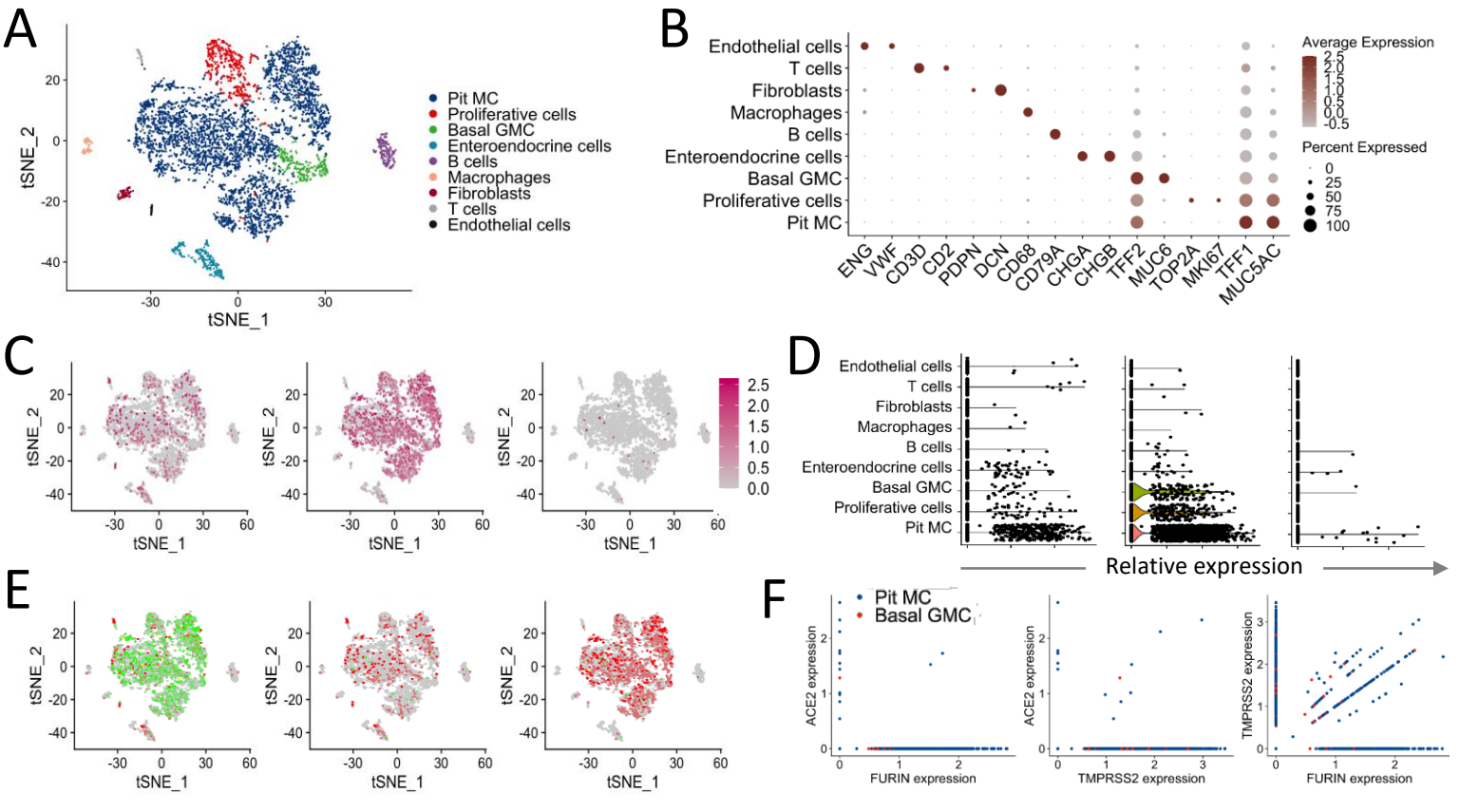


Single-cell RNA profiling of human gastric tissue

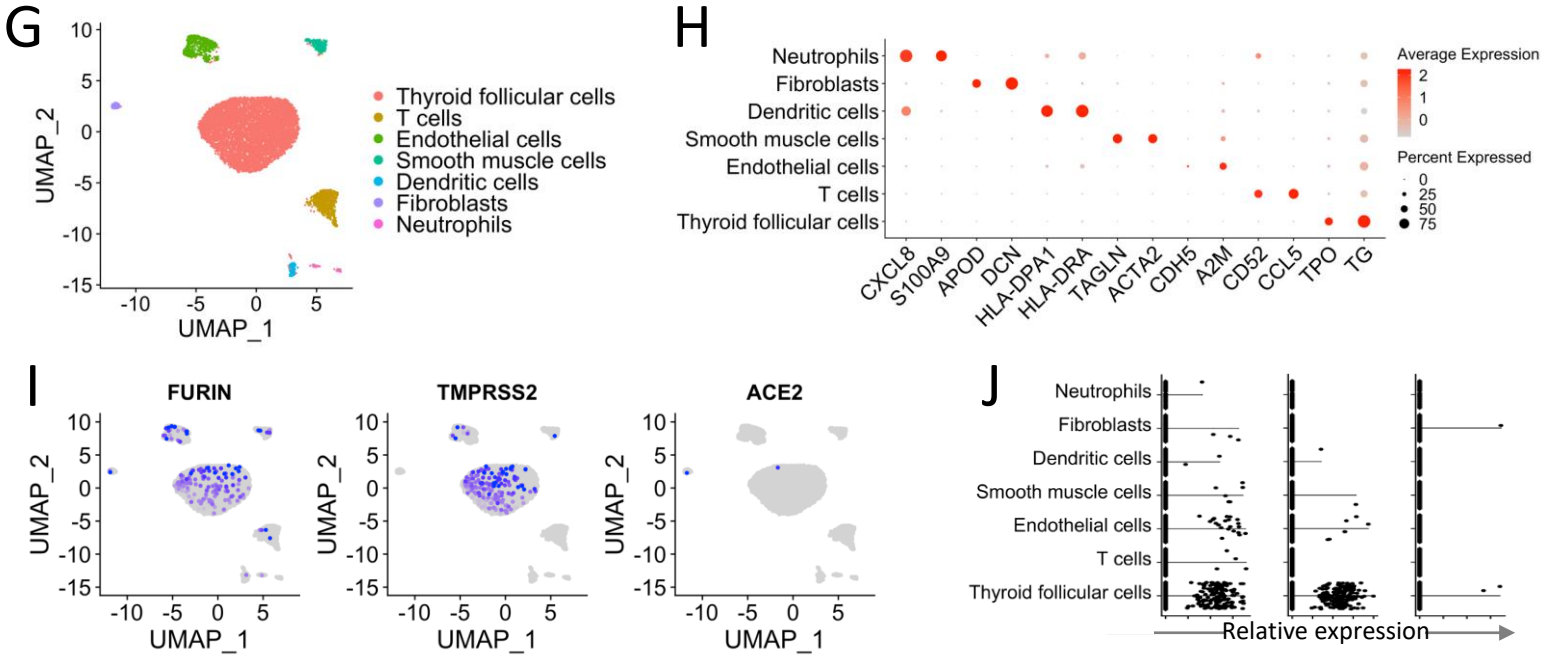


Single-cell RNA profiling of human thyroid gland

Figure S3